Clinical Microbiology and Infection xxx (xxxx) xxx

Contents lists available at ScienceDirect

Clinical Microbiology and Infection

journal homepage: www.clinicalmicrobiologyandinfection.com

Original article

The effects of single and multiple resistance mechanisms on bacterial response to meropenem

Dominika T. Fuhs [1, †], Sara Cortés-Lara [2, 3, †], Jessica R. Tait [1], Kate E. Rogers [1], Carla López-Causapé [2, 3], Wee Leng Lee [1], David M. Shackleford [4], Roger L. Nation [1], Antonio Oliver [2, 3, §], Cornelia B. Landersdorfer [1, *, §]

[1] Drug Delivery, Disposition and Dynamics, Monash Institute of Pharmaceutical Sciences, Monash University, Parkville, VIC, Australia
[2] Servicio de Microbiología, Hospital Universitario Son Espases, Instituto de Investigación Sanitaria Illes Balears (IdISBa), Palma de Mallorca, Spain
[3] CIBER Enfermedades Infecciosas (CIBERINFEC), Madrid, Spain
[4] Centre for Drug Candidate Optimisation, Monash Institute of Pharmaceutical Sciences, Monash University, Parkville, VIC, Australia

ARTICLE INFO

Article history:
Received 1 March 2024
Received in revised form
27 May 2024
Accepted 26 June 2024
Available online xxx

Editor: W. Couet

Keywords:
Antibiotic resistance
Population genomics
Pseudomonas aeruginosa
Quantitative systems pharmacology
Whole genome sequencing

ABSTRACT

Objectives: Meropenem is commonly used against *Pseudomonas aeruginosa*. Traditionally, the time unbound antibiotic concentration exceeds the MIC ($fT_{>MIC}$) is used to select carbapenem regimens. We aimed to characterize the effects of different baseline resistance mechanisms on bacterial killing and resistance emergence; evaluate whether $fT_{>MIC}$ can predict these effects; and, develop a novel Quantitative and Systems Pharmacology (QSP) model to describe the effects of baseline resistance mechanisms on the time-course of bacterial response.

Methods: Seven isogenic *P. aeruginosa* strains with a range of resistance mechanisms and MICs were used in 10-day hollow-fiber infection model studies. Meropenem pharmacokinetic profiles were simulated for various regimens ($t_{1/2,meropenem}$ = 1.5 h). All viable counts on drug-free, 3 × MIC, and 5 × MIC meropenem-containing agar across all strains, five regimens, and control (n = 90 profiles) were simultaneously subjected to QSP modeling. Whole genome sequencing was completed for total population samples and emergent resistant colonies at 239 h.

Results: Regimens achieving ≥98%$fT_{>1 \times MIC}$ suppressed resistance emergence of the *mexR* knockout strain. Even 100%$fT_{>5 \times MIC}$ failed to achieve this against the strain with OprD loss and the *ampD* and *mexR* double-knockout strain. Baseline resistance mechanisms affected bacterial outcomes, even for strains with the same MIC. Genomic analysis revealed that pre-existing resistant subpopulations drove resistance emergence. During meropenem exposure, mutations in *mexR* were selected in strains with baseline *oprD* mutations, and *vice versa*, confirming these as major mechanisms of resistance emergence. Secondary mutations occurred in *lysS* or *argS*, coding for lysyl and arginyl tRNA synthetases, respectively.

Discussion: The QSP model well-characterized all bacterial outcomes of the seven strains simultaneously, which $fT_{>MIC}$ could not. **Dominika T. Fuhs, Clin Microbiol Infect 2024;▪:1**

Introduction

Carbapenem-resistant *Pseudomonas aeruginosa* causes high mortality in intensive care units [1,2]. *P. aeruginosa* is among the leading pathogens causing deaths associated with antimicrobial resistance worldwide [3].

Antibiotic development cannot keep up with the rise in antimicrobial resistance and resistance emerges rapidly even against

* Corresponding author. Cornelia B. Landersdorfer, Drug Delivery, Disposition and Dynamics, Faculty of Pharmacy and Pharmaceutical Sciences, Monash University, Parkville, Australia.
E-mail address: cornelia.landersdorfer@monash.edu (C.B. Landersdorfer).
† These authors contributed equally (joint first co-authors) to this work: Dominika T. Fuhs, Sara Cortés-Lara.
§ These authors contributed equally (joint senior co-authors) to this work: Antonio Oliver, Cornelia B. Landersdorfer.

https://doi.org/10.1016/j.cmi.2024.06.026

Table 1
Isogenic strains of *P. aeruginosa* and their baseline MICs

Strain	Description	MIC_{MEM} (mg/L)*	Susceptibility to MEM#	Ref.
PAO1	Wild-type reference strain	1	S	—
PAΔAD	*ampD* knockout resulting in AmpC overexpression	2	S	[18]
PAΔmexR	*mexR* knockout resulting in overexpression of MexAB-OprM efflux	4	I	[21]
PAOD1	Spontaneous *oprD* mutant resulting in the loss of OprD porin channels	4	I	[19]
PAΔDΔmexR	*ampD* and *mexR* knockout	4	I	[21]
PAOD1ΔmexR	Spontaneous *oprD* mutant and *mexR* knockout	16	R	[21]
PAOD1ΔD	Spontaneous *oprD* mutant and *ampD* knockout	16	R	[19]

Δ: deletion, MEM: meropenem, *determined by agar dilution [20] #according to CLSI clinical breakpoints, S: susceptible, I: intermediate, R: resistant. All isogenic strains were constructed from PAO1 by the group of Antonio Oliver, Instituto de Investigación Sanitaria Illes Balears.

new compounds [4,5]. Therefore, there is a pressing need for new approaches to describe and predict resistance emergence during antibiotic exposure and optimize antibiotic dosing regimens [6]. Traditionally, pharmacokinetic/pharmacodynamic (PK/PD) indices have linked antibiotic exposure with bacterial response and informed dosing [7,8]. For carbapenems the relevant PK/PD index is the percentage of time during which unbound antibiotic concentrations exceed the MIC over 24h ($\%fT_{>MIC}$) [9]. However, limitations of these indices are increasingly recognized, including that they do not capture the full time-courses of antibiotic PK and bacterial response, do not appropriately account for resistance emergence, and use MIC as a PD measure of drug potency [6,10]. In contrast, mechanism-based PK/PD and Quantitative and Systems Pharmacology (QSP) models describe and predict the full time-courses of bacterial growth, killing, and resistance emergence [11,12].

P. aeruginosa possesses an exceptional ability for resistance emergence during antibiotic treatment [13,14]. Carbapenem resistance may be attributed to OprD porin channel inactivation, efflux pump hyperproduction, production of antibiotic-deactivating enzymes, or combinations thereof [15]. Currently, there is a lack of knowledge on the impact of various *P. aeruginosa* baseline resistance mechanisms, i.e. which are present pre-treatment, on bacterial killing and resistance emergence during treatment. We used meropenem, commonly administered in intensive care units against *P. aeruginosa*, as a probe to explore this issue [1,16]. Published meropenem PK/PD models for *P. aeruginosa* did not directly incorporate the effects of baseline bacterial characteristics on resistance emergence [17]. To our knowledge, no studies have employed an integrated experimental and modeling approach to systematically investigate meropenem regimens in the context of different resistance mechanisms using a panel of isogenic strains.

This study aimed to (a) characterize the effect of different meropenem regimens on bacterial killing and resistance emergence in seven isogenic *P. aeruginosa* strains with one or multiple baseline resistance mechanisms, (b) identify genetic changes in bacteria relating to resistance emergence during meropenem exposure, (c) assess whether observed bacterial responses are consistent with the $\%fT_{>MIC}$, and (d) develop a QSP model that quantitatively describes effects of baseline resistance mechanisms on bacterial killing and resistance emergence across strains.

Materials and methods

Strains and susceptibility testing

The *P. aeruginosa* wild-type reference strain PAO1 and six isogenic strains constructed from PAO1 (PAΔAD, PAOD1, PAΔmexR, PAΔDΔmexR, PAOD1ΔmexR, and PAOD1ΔD) were studied (Table 1; [18–21]). The only differences between PAO1 and its isogenic strains were the introduced resistance mechanisms. This allowed for a direct investigation of the impact of these resistance mechanisms on bacterial response. The meropenem MIC before antibiotic exposure and baseline $\log_{10}$ mutant frequency ($\log_{10}$MF) were determined for all strains in biological replicates on different days (described in Supplementary materials).

Dynamic hollow-fiber infection model studies

The hollow-fiber infection model (HFIM) exposed the strains to free meropenem concentration–time profiles reflecting the PK in critically ill patients with normal renal function (CL_{CR} = 120 mL/min, meropenem $t_{1/2}$ = 1.5 h) [22,23], following clinically-relevant dosing regimens listed in Table 2 [24–26]. Untreated controls were included for each strain. Details of HFIM studies are described in Supplementary materials.

Whole genome sequencing and analysis of emergent meropenem resistance mechanisms

Total population samples and saved colonies that grew on 5 × MIC meropenem-containing agar, obtained from the HFIM at 239 h for PAO1 and each isogenic strain and dosing regimen (including controls), were fully sequenced. Details are described in Supplementary materials.

Quantitative and systems pharmacology modeling

A QSP model was developed to account for bacterial growth, killing, and resistance emergence for all five regimens and seven strains simultaneously, importantly without estimating strain-specific drug effect parameters. The model was informed by the total and less-susceptible bacterial counts, baseline resistance mechanisms, and genome sequencing. It explained the bacterial

Table 2
Meropenem (MEM) regimens (and mode of administration) simulated in the hollow-fiber infection model against seven isogenic *P. aeruginosa* strains

MEM regimens	Isogenic strains (number of biological replicates)
1 g, Q8h	PAO1 (1), PAΔAD (1), PAΔmexR (1), PAOD1 (1), PAΔDΔmexR (1)
2 g, Q8h	PAΔmexR (1), PAOD1 (1), PAΔDΔmexR (1)
3 g/d, CI	PAO1 (1), PAΔAD (1), PAΔmexR (1), PAOD1 (1), PAΔDΔmexR (1)
6 g/d, CI	PAΔmexR (1), PAOD1 (2), PAΔDΔmexR (3), PAOD1ΔmexR (1), PAOD1ΔD (2)
12 g/d, CI	PAΔmexR (1), PAOD1 (1), PAΔDΔmexR (1), PAOD1ΔmexR (1), PAOD1ΔD (2)

CI, continuous infusion; Q8h, 3-h infusion administered 8-hourly.
Since the standard 1 g Q8h and 3 g daily CI meropenem dosing regimens resulted in bacterial killing and suppression of the emergence of resistance for PAO1 and PAΔAD strains, higher meropenem dosing regimens were not tested against these strains. The higher-than-approved 12 g/d CI was included to reflect meropenem doses and concentrations related to high-dose regimens and to further explore the concentration–effect relationship for the meropenem-resistant strains [24].

Please cite this article as: Fuhs DT et al., The effects of single and multiple resistance mechanisms on bacterial response to meropenem, Clinical Microbiology and Infection, https://doi.org/10.1016/j.cmi.2024.06.026

outcomes by incorporating the effects of different resistance mechanisms on the estimated meropenem concentration at the site of action (periplasmic space) which drives bacterial response. See Supplementary materials for details, including a schematic diagram.

Ethics: not applicable.

Results

MICs and baseline mutant frequencies

The strains encompassed a wide range of meropenem susceptibilities (Table 1). The baseline $\log_{10}$MFs indicated the presence of a small proportion of pre-existing less-susceptible bacterial subpopulations in the overall population of each strain (Table S1).

HFIM studies

The observed meropenem concentrations following continuous infusion (CI) were on average within 4% of the target. The targeted concentrations for the 3 h intermittent infusions every 8 h (Q8h) were also well replicated (Fig. S1). All strains grew well in the untreated controls (Fig. 1), and less-susceptible populations growing on 3 × and 5 × MIC meropenem-containing agar plateaued at ~3–4 $\log_{10}$ CFU/mL by ~24 h, except for PAO1 that plateaued from ~48 h (Fig. 2; Fig. S2).

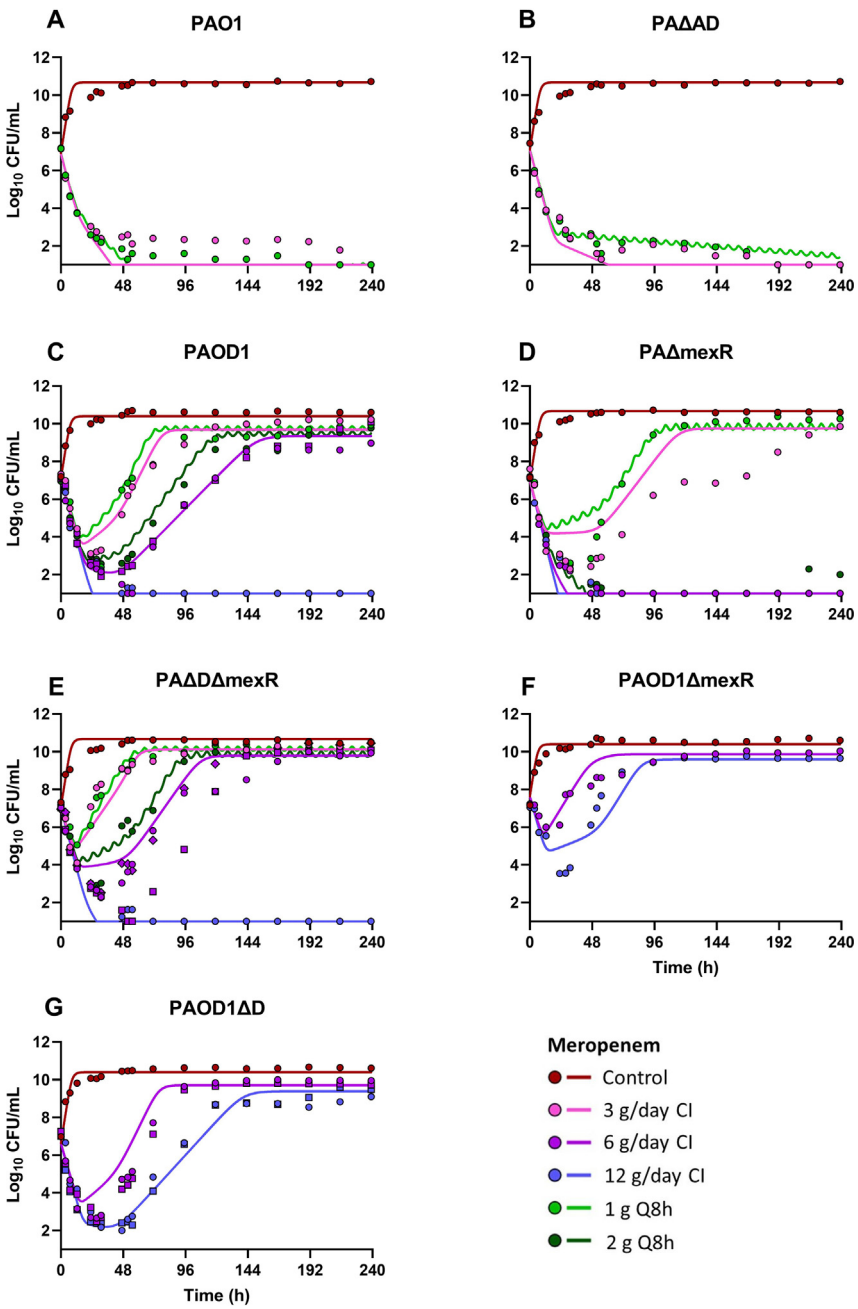

Fig. 1. Total bacterial population (observed viable counts in symbols, and population predicted profiles of the QSP model in lines in corresponding colors) vs. time. The *y*-axis starts at the limit of counting = 1 $\log_{10}$ CFU/mL. $n = 1–3$, biological replicates are shown as different symbols. The population fits overpredicted the temporary plateau at ~96 h–168 h for PAΔmexR and 3 g/d CI. For the 6 g/d CI against PAΔDΔmexR, the model well described two biological replicates, while regrowth of the third replicate occurred slightly later.

Please cite this article as: Fuhs DT et al., The effects of single and multiple resistance mechanisms on bacterial response to meropenem, Clinical Microbiology and Infection, https://doi.org/10.1016/j.cmi.2024.06.026

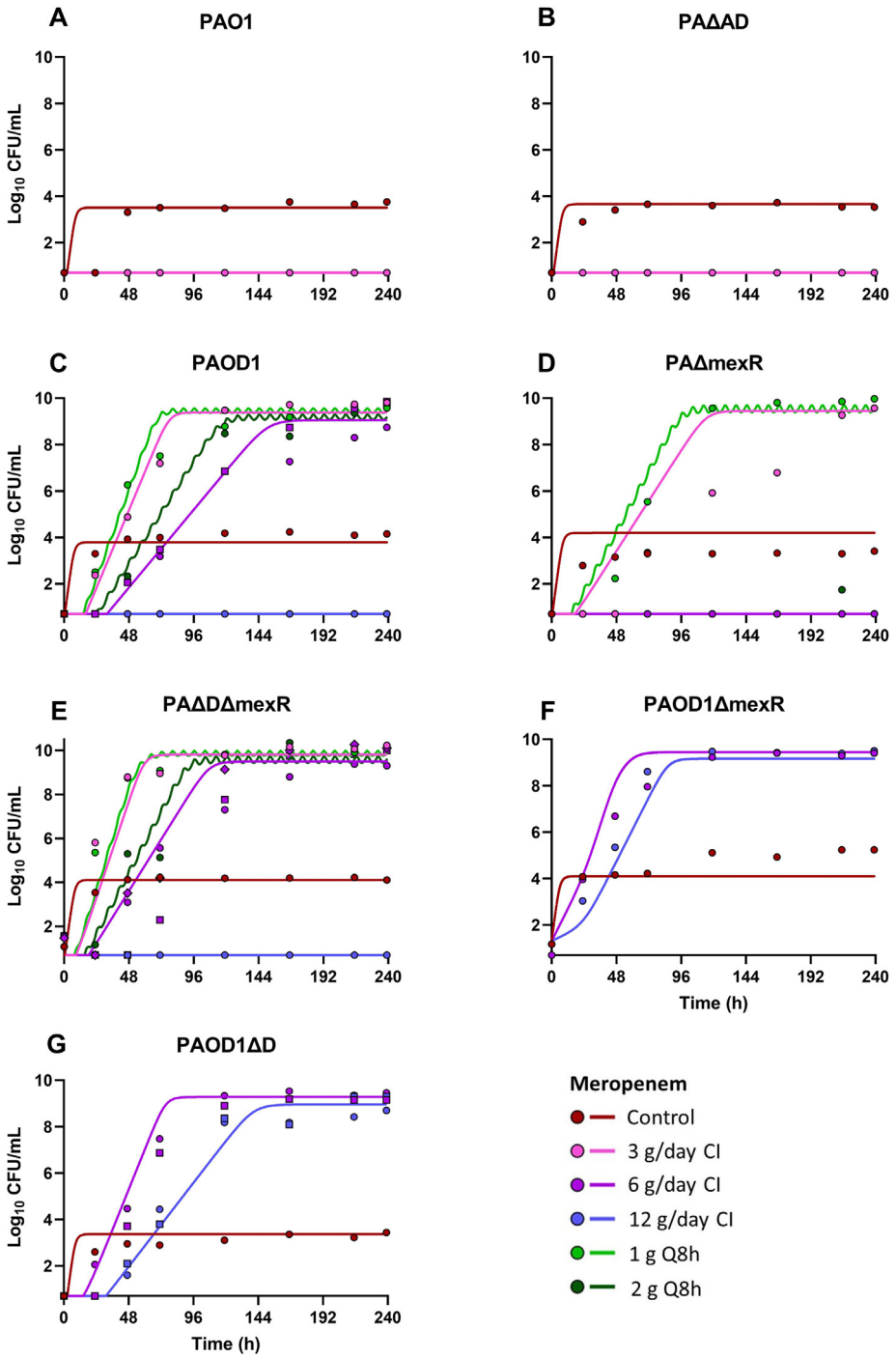

Fig. 2. Less-susceptible bacterial population growing on 3 × MIC MEM-containing drug plates (observed viable counts in symbols, and population predicted profiles of the QSP model in lines in corresponding colors) vs. time. The *y*-axis starts at the limit of counting = 0.7 $\log_{10}$ CFU/mL. n = 1–3, biological replicates are shown as different symbols.

PAO1 and PAΔAD

Exposure to 3 g/day CI and 1g Q8h regimens (≥98%$fT_{>1 \times MIC}$) caused ≥5 $\log_{10}$ CFU/mL killing and suppressed resistance emergence (Fig. 1a and b), with less-susceptible bacteria not detected for either strain (Fig. 2a and b; Fig. S2a and b). No effect of the *ampD* mutation was observed when comparing PAΔAD to PAO1, despite slightly different baseline MICs.

PAΔmexR, PAOD1, and PAΔDΔmexR

The lowest CI and Q8h regimens resulted in bacterial regrowth with resistance emergence for all three strains (Figs. 1c–e), although the CI achieved 100%$fT_{>2 \times MIC}$. Regrowth of the PAΔDΔmexR double mutant occurred substantially faster (from ~23 h) compared with the other two strains. The 6 g/day CI (100%$fT_{>5 \times MIC}$) and 2g Q8h (98%$fT_{>1 \times MIC}$) regimens produced ≥5 $\log_{10}$ CFU/mL killing and suppressed regrowth of less-susceptible bacteria only against PAΔmexR. Despite having the same MIC as PAΔmexR, the PAOD1, and PAΔDΔmexR displayed extensive regrowth with resistance emergence (Fig. 2c and e; Fig. S2c and e; Table S2). The addition of the *ampD* mutation to the *mexR* mutation in PAΔDΔmexR substantially affected bacterial response, as the two resistance mechanisms acted synergistically against meropenem.

Please cite this article as: Fuhs DT et al., The effects of single and multiple resistance mechanisms on bacterial response to meropenem, Clinical Microbiology and Infection, https://doi.org/10.1016/j.cmi.2024.06.026

Only the 12 g/day CI ($100\%fT_{>10 \times MIC}$) produced bacterial eradication and suppressed resistance emergence of all three strains.

PAOD1ΔmexR and PAOD1ΔD

The 6 g/day CI ($100\%fT_{>1 \times MIC}$) achieved only ~1 $\log_{10}$ CFU/mL killing of PAOD1ΔmexR before almost immediate regrowth with resistance emergence. The same regimen produced ~5 $\log_{10}$ CFU/mL initial bacterial killing of PAOD1ΔD before regrowth of less-susceptible bacteria, although both strains had the same MIC. Even 12 g/day CI ($100\%fT_{>2 \times MIC}$) was unable to suppress the regrowth and resistance emergence of either strain (Fig. 1f and g; Fig. 2f and g; Fig. S2f and g).

All strains

All treatments resulting in regrowth amplified resistance with bacterial counts above the baseline resistance shown in control populations (Fig. 2; Fig. S2). Overall, 3-hour infusions Q8h performed similarly to CI at a given daily dose, with trends of a slightly better performance of the 3 g CI against PAΔmexR, and the 6 g CI against PAOD1 and PAΔDΔmexR.

Whole genome sequencing and analysis of emergent meropenem resistance mechanisms

The mutations detected at 239 h in total population samples and individual colonies that grew on meropenem-containing agar are presented in Table 3. All analysed colonies retained resistance (supported by significantly increased meropenem MICs, Table 3) after culturing in drug-free media. Following the HFIM studies, several of the isogenic strains exhibited additional mutations in genes known to be responsible for meropenem resistance. In general, mutations in *mexAB* regulators (resulting in MexAB-OprM efflux pump overexpression) were detected in isogenic strains with baseline *oprD* mutation. Mutations in *oprD* (resulting in OprD porin inactivation) were detected in isogenic strains with baseline *mexR* mutations. Secondary mutations occurred mostly in *lysS* or *argS*, coding for lysyl and arginyl tRNA synthetases, respectively. Other genes found to be mutated in more than one experiment included *alaS* (alanyl-tRNA synthetase), *phoQ* (two-component sensor PhoQ), *spoT* (guanosine-3′,5′-bis(diphosphate) 3′-pyrophosphohydrolase) and *aroB* (3-dehydroquinate synthase). A large genomic deletion of the *galU* region was detected in a single colony from a PAΔmexR control, and a PBP3 (F533L) mutation in a single colony from 1 g Q8h treatment of PAΔDΔmexR.

QSP modeling

In this model, amplification of small pre-existing resistant subpopulations with additional resistance mutations compared with the baseline resistome of the respective strain, drove bacterial regrowth and resistance emergence, supported by the genomic analysis. The model yielded unbiased and sufficiently precise fits for the total and less-susceptible bacterial counts for all strains; demonstrated by the population-fitted curves without random variability (Figs. 1, 2 and S2) and the goodness-of-fit plots (Fig. S3). All regimens and controls across all strains were described simultaneously by the same model and largely the same parameter estimates (Table S3). Distinct parameter estimates were required only to describe the observed differences in initial inocula and the proportions of pre-existing bacterial subpopulations between strains (Table S4). Differences in bacterial killing and resistance emergence among strains were characterized mainly by the effects of a given resistance mechanism/s present in the strains. All standard errors of parameter estimates were <16%, indicating excellent precision. The model very well described up to five different treatments and control arms for each of seven isogenic strains and their biological replicates (including total and less-susceptible subpopulations), i.e. in total 90 curves modeled simultaneously.

Discussion

For carbapenems, traditional PK/PD targets of $40\%fT_{>1 \times MIC}$ from preclinical studies, and $75\%fT_{>1 \times MIC}$ from clinical studies, have been linked to maximum bacterial killing and clinical cure, respectively [27]. Targets of $100\%fT_{>1 \times MIC}$ and $100\%fT_{>4\text{-}6 \times MIC}$ have been proposed for severe infections in critically ill patients [28], and suppressing resistance emergence, respectively [29,30]. Across our HFIM studies, $\%fT_{>MIC}$ alone could not predict bacterial outcomes; demonstrating the PK/PD relationship was more complex than $\%fT_{>MIC}$. Even at the same MIC, the baseline resistance mechanism could affect the meropenem regimen required to suppress regrowth and resistance emergence.

Our results are instructive regarding the effect of two pre-existing resistance mechanisms working together to influence bacterial response, including resistance emergence during meropenem exposure. The lowest CI and Q8h regimens achieved substantial bacterial killing and suppressed resistance emergence against PAO1 and PAΔAD. Thus, the *ampD* mutation had little effect on the bacterial outcome as a single resistance mechanism in PAΔAD compared with PAO1. This is not surprising since the *ampD* mutation has not been shown to substantially impact carbapenem effectiveness [31]. In addition, whole genome sequencing revealed *oprD* mutational inactivation and MexAB-oprM overexpression through mutation of its negative regulators *mexR* or *nalD* were the primary mechanisms of meropenem resistance amplified during therapy. In contrast, mutations in *ampD* (or other *ampC* regulators such as *dacB* or *ampR*) were not amplified by meropenem exposure, indicating AmpC overexpression plays a minor role against meropenem effectiveness. Frequently selected mutations in aminoacyl tRNA synthetases likely reflect fitness cost compensatory mutations of the inactivation of *oprD*, coding for a porin involved in basic amino acids uptake [32]. The bacterial response changed substantially when the *ampD* mutation was paired with a mutation resulting in increased efflux pumps (*mexR*) in PAΔDΔmexR as compared with PAΔmexR. Similarly, the addition of the *ampD* mutation to the *oprD* mutant enhanced resistance. Although 12 g/day CI suppressed resistance emergence of PAOD1 over 10 days, this regimen resulted in substantial resistance emergence in PAOD1ΔD from ~3 days onwards. This highlights the importance of the interplay between multiple resistance mechanisms.

In contrast to $\%fT_{>MIC}$, our QSP model well-characterized bacterial responses across all strains simultaneously, by accounting not only for the effects of different baseline resistance mechanisms but also their interplay. Among single mutations, *oprD* had the largest effect on meropenem resistance, followed by *mexR*. Similar to our study findings, OprD porin inactivation was reported as the resistance mechanism conferring the highest level of meropenem resistance in *P. aeruginosa* clinical isolates [33]. Moreover, the model well described the effects of combinations of resistance mechanisms in double mutant strains, which notably included the observed enhancement effects of *ampD* plus *mexR* mutations. Current semi-mechanistic models may include bacterial phenotypic characteristics but do not directly include bacterial genomic characteristics such as resistance mechanisms. Typically, available models fit data from one, or up to three, strains in the same dataset. If multiple strains are present in the model, the differences in response to studied antibiotic(s) are frequently characterized by different parameter estimates for drug effect for each strain [17,34]. These drug effect parameters are most often not informed by genomic characteristics; therefore, are not predictable and

Please cite this article as: Fuhs DT et al., The effects of single and multiple resistance mechanisms on bacterial response to meropenem, Clinical Microbiology and Infection, https://doi.org/10.1016/j.cmi.2024.06.026

Table 3
Mutations detected in total population samples and saved colonies of isogenic strains of *P. aeruginosa* after the completion of treatment in the hollow-fiber infection model (239 h)

Strain [MIC mg/L, basal resistome]	Dosing regimen tested (biological replicate)	Genomic mutations (frequency detected %) in total population sample	Colony 1		Colony 2	
			MIC (mg/L)	Genomic mutations detected	MIC (mg/L)	Genomic mutations detected
PAOD1	Control		16	*alaS* (V670L)	8-16	
[4 mg/L, *oprD* W65X]	3 g CI	*mexR* (nt165Δ11 85%), *rne* (aa419insSL 71.4%)	32	*mexR* (nt165Δ11), *rne* (aa419insSL)	32	*mexR* (nt165Δ11), *rne* (aa419insSL)
	6 g CI (1)	*mexR* (I68F 18.4%), *nalD* (T11N 1.7%), *lysS* (G213A 10.3%)	128	*nalD* (T11N), *lysS* (G213A)	256	*mexR* (I68F)
	6 g CI (2)	*nalD* (T158P 3.4%), *lysS* (K152M 22%, P269L 73%), *mpl* (nt112InsC 4.3%)	32	*lysS* (K152M), *mpl* (nt112InsC)	64	*nalD* (T158P), *lysS* (P269L)
	1 g Q8h	*mexR* (G58E 4.4%), *alaS* (aa414Δ2 84.9%)	64	*mexR* (G58E), *alaS* (aa414Δ2)	64	*mexR* (G58E), *alaS* (aa414Δ2)
	2 g Q8h	*mexR* (L43 × 1.75%, F93I 18.6%), *lysS* (G213A 97.5%)	128	*mexR* (F93I), *lysS* (G213A)	64	*mexR* (L43X), *lysS* (G213A)
PAΔmexR [4 mg/L, *mexR* nt136Δ205]	Control		32	*azoR* (nt445Δ1, nt449Δ1), *mexZ* (deleted), *mexY* (deleted), *mexX* (deleted), *galU* (deleted), PA2217 (nt1Δ184), *copS* (nt539InsCGGA)	8	*copS* (nt966Δ367)
	3 g CI	*oprD* (W138 × 7.4%); *phoQ* (nt2001Δ28 12.8%)	32	*phoQ* (nt2001Δ28)[a]	32	*oprD* (W138X)
	1 g Q8h	*oprD* (Q166 × 99.8%), *aroB* (Y116 × 9.5%)	64	*oprD* (Q166X), *aroB* (Y116X)	64	*oprD* (Q166X), *aroB* (Y116X)
PAΔDΔmexR	Control		32	*oprD* (nt1206InsC)	32	*oprD* (W277X)
[4 mg/L, *ampD* nt1Δ169, *mexR* nt136Δ205]	3 g CI	*oprD* (nt582InsGA 14.2%), *rpoB* (R457C 1.7%), *mraY* (N221T 9,1%)	64	*oprD* (nt582InsGA), *mraY* (N221T)	64	*oprD* (nt563Δ161), *rpoB* R457C
	6 g CI (1)	*oprD* (nt827Δ4 98%)	128	*oprD* (nt827Δ4)	128	*oprD* (nt827Δ4)
	6 g CI (2)	*oprD* (nt636InsG 83.7%), *phoQ* (V260G 1%), *rpsK* (aa92InsGP 15.2%), *spoT* (aa126Δ2 < 1%)	128	*oprD* (nt636InsG), *phoQ* (V260G)[a], *spoT* (aa126Δ2)	64	*oprD* (nt636InsG), *rpsK* (aa92InsGP)
	6 g CI (3)	Low-quality sequence*	128	*oprD* (nt636InsG), *spoT* (aa128InsMA)	128	*oprD* (nt636InsG), *spoT* (nt1660Δ7)
	1 g Q8h	*oprD* (nt1206InsC 28.6%), *mraY* (I161N 4.3%)	64	*oprD* (nt563Δ161), *mraY* (I161N), PA4685 (nt1Δ641)	128	*oprD* (nt1206InsC), *ftsI* (F533L)
	2 g Q8h	*oprD* (G307D 8.7%, nt827Δ4 88.8%), *spoT* (nt410Δ1 3.5%, aa126Δ2 14.4%)	128	*oprD* (G307D), *spoT* (nt410Δ1)	128	*oprD* (nt827Δ4), *spoT* (aa126Δ2)
PAOD1ΔmexR	Control		128	*aspS* (R334H)	64	PA2607 (T4P)
[16 mg/L, *oprD* W65X, *mexR* nt136Δ205]	6 g CI	*lysS* (R489C 17.9 %), *aroB* (S131P 39.7%)	128	*rne* (F57V), *aroB* (S131P)	64	*lysS* (R489C)
	12 g CI	*lysS* (R498C 51.2 %)	256	*lysS* (R498C)	128	*lysS* (R498C)
PAOD1ΔD	Control		64	*argS* (T476P)	-	
[16 mg/L, *oprD* W65X, *ampD* nt1Δ169]	6 g CI (1)	*argS* (L189Q 6.9%), PA2775.1 (T25A 51.6%)	128	*argS* (L189Q)	256	PA2775.1 (T25A)
	6 g CI (2)	*argS* (V164I 21.2%)	128	*mexR* (G101E), *argS* (V164I)	64	*argS* (V164I)
	12 g CI (1)	*mexR* (G58E 8.8%, R70Q <1%), *argS* (F86L 66.8%)	256	*mexR* (G58E), *argS* (F86L)	256	*mexR* (R70Q), *argS* (F86L)
	12 g CI (2)	*mexR* (L95P 32.9%), *argS* (A468V 66.4%)	256	*mexR* (L95P), *argS* (A468V)	256	*mexR* (L95P), *argS* (A468V)

[a] phoQ mutants IDEA01-G-1 (nt2001Δ28, 16 mg/L) and IDEA04-B-1 (V260G, 2 mg/L) additionally showed increased colistin MICs as compared with parent strains (0.5 mg/L).

translatable across strains. In contrast, our novel model was informed by knowledge of key bacterial characteristics and allowed for quantification of effects of pre-existing resistance mechanisms on antibiotic success and characterization of the interaction between resistance mechanisms, with the same parameter estimates of drug effect across strains.

Our results suggest resistance mechanisms of the isogenic strains (*oprD*, *mexR*, *ampD*) when combined with a second mutation reduced bacterial killing, thus allowing for the selection and amplification of pre-existing mutants with additional resistance mutations, which were responsible for driving regrowth and resistance emergence. The constant concentrations of such subpopulations in the control arms of each strain (detectable from 1-2 days onwards when the total population had reached a plateau) strongly suggest their presence pre-treatment. Furthermore, there was an overlap between mutations seen in the colonies from the control and the colonies from treated arms for most strains, consistent with the assumption of amplification of pre-existing resistant mutants. The *aspS* mutation in the PAOD1ΔmexR control colony can be considered equivalent to the *lysS* mutations in the treatment arms [35,36]. In PAΔmexR a commonly occurring large genomic deletion in *galU* caused resistance in a control mutant but

Please cite this article as: Fuhs DT et al., The effects of single and multiple resistance mechanisms on bacterial response to meropenem, Clinical Microbiology and Infection, https://doi.org/10.1016/j.cmi.2024.06.026

was not selected by treatment because of its higher fitness cost compared with the *oprD* mutation which was selected by treatment [37]. Thus, sequencing results (in addition to baseline $\log_{10}$MFs) supported the model assumption that pre-existing resistant subpopulations drove the regrowth. In the model, the baseline resistance mutations decreased meropenem concentrations in the periplasmic space, allowing for the selection and amplification of pre-existing mutants with increased resistance to meropenem.

Standard, culture-dependent antimicrobial susceptibility testing is labour-intensive and often requires several days, which may delay the selection of appropriate therapy [38,39]. Thus, many patients are still being treated empirically, often leading to poor outcomes and increased resistance [40,41]. Currently, with the increasing burden of antimicrobial resistance, rapid whole genome sequencing-based diagnostic testing is an option that could allow for the identification of the infecting pathogen including the detection of resistance genes [42]. By identifying resistance characteristics, a therapy adapted to the individual pathogen (and patient) is an exciting prospect. Future studies to expand our novel model to clinical isolates and antibiotic combinations are warranted. Ultimately, coupling such an expanded model with genomic analysis could represent a necessary first step towards model-informed personalized antibiotic regimens against *P. aeruginosa* infections [11].

To our knowledge, this study is the first to investigate the response to meropenem in the context of *P. aeruginosa* resistance mechanisms in an HFIM, followed by the development of a novel QSP model. The isogenic strains reflected important resistance mechanisms common in clinical isolates [14,21]. Biological replicates ensured the reproducibility of results. The quantification of resistant subpopulations on 3 × and 5 × MIC meropenem-containing agar enabled incorporating them in the model and investigating resistance emergence. Genome sequencing of resistant colonies provided detailed insights into mechanisms of resistance emergence during meropenem exposure. In our study, meropenem in the periplasmic space was not measured. However, utilizing isogenic strains allowed for accurate estimation of the effects of different resistance mechanisms on bacterial response for each strain and regimen. Since the effects are driven by meropenem concentrations at the site of action (periplasmic space) in the isogenic strains compared with PAO1, an accurate estimate of the permeation rate or the nominal values of concentrations at the site of action was not required for the purpose of the current analysis. There is a paucity of information available on the rate of outer membrane permeability of meropenem in *P. aeruginosa* [43]; as more becomes available the model could be extended. Similar to other *in vitro* models, the HFIM lacks an immune system; therefore, the observed bacterial responses may best reflect meropenem effects as could be seen in immunosuppressed patients.

In summary, the pharmacodynamic response was more complex than could be explained by $\%fT_{>MIC}$. We showed that even for strains with the same MIC, baseline resistance mechanisms affected bacterial outcomes and the meropenem regimens required to suppress regrowth and resistance emergence. The model well-characterized the responses of seven isogenic strains simultaneously. The novel QSP model represents a step towards a better understanding of the complicated relationship between antibiotics, bacterial characteristics, and resistance emergence during treatment. This investigation provided a potential future approach towards enabling optimized antibiotic therapy.

Author contributions

CBL conceptualized and designed the study with input from AO and RLN. DTF, SC-L, JRT, KER, and WLL conducted the study. DTF, SC-L, and JRT analysed the data. JRT, CL-C, DMS, AO, and CBL provided supervision. CBL, AO, and RLN acquired the funding. AO provided resources. DTF wrote the original draft of the manuscript. SC-L, JRT, CL-C, DMS, RLN, AO, and CBL reviewed and edited the manuscript. All authors provided feedback and approved the final version.

Transparency declaration

The authors declare that they have no conflicts of interest. This work was supported by the Australian National Health and Medical Research Council (NHMRC) Ideas grant GNT1184428 to CBL, AO, and RLN; DTF and JRT were supported by NHMRC Centre of Research Excellence GNT2007007 to CBL, and DTF by a Monash Graduate Scholarship.

Sequence information

European Nucleotide Archive project number: PRJEB71060.

Acknowledgements

Parts of the experimental data in this work were presented as an oral presentation at the 33rd European Congress of Clinical Microbiology and Infectious Diseases (ECCMID) in Copenhagen, Denmark, 15–18 April 2023, and an ePoster flash presentation at ESCMID Global in Barcelona, Spain, 27–30 April 2024.

Appendix A. Supplementary data

Supplementary data to this article can be found online at https://doi.org/10.1016/j.cmi.2024.06.026.

References

[1] Gill CM, Nicolau DP. Carbapenem-resistant *Pseudomonas aeruginosa*: an assessment of frequency of isolation from ICU versus non-ICU, phenotypic and genotypic profiles in a multinational population of hospitalized patients. Antimicrob Resist Infect Control 2022;11:146.
[2] MacVane SH. Antimicrobial resistance in the intensive care unit: a focus on gram-negative bacterial infections. J Intensive Care Med 2016;32:25–37.
[3] Murray CJL, Ikuta KS, Swetschinski L, Robles Aguilar G, Gray A, Han C, et al. Global burden of bacterial antimicrobial resistance in 2019: a systematic analysis. Lancet 2022;399:629–55.
[4] Butler MS, Gigante V, Sati H, Paulin S, Al-Sulaiman L, Rex JH, et al. Analysis of the clinical pipeline of treatments for drug-resistant bacterial infections: despite progress, more action is needed. Antimicrob Agents Chemother 2022;66:e0199121.
[5] Theuretzbacher U, Outterson K, Engel A, Karlén A. The global preclinical antibacterial pipeline. Nat Rev Microbiol 2020;18:275–85.
[6] Rao GG, Landersdorfer CB. Antibiotic pharmacokinetic/pharmacodynamic modelling: MIC, pharmacodynamic indices and beyond. Int J Antimicrob Agents 2021;58:106368.
[7] Friberg LE. Pivotal role of translation in anti-infective development. Clin Pharmacol Ther 2021;109:856–66.
[8] Drusano GL. Antimicrobial pharmacodynamics: critical interactions of 'bug and drug'. Nat Rev Microbiol 2004;2:289–300.
[9] Craig WA. Pharmacokinetic/pharmacodynamic parameters: rationale for antibacterial dosing of mice and men. Clin Infect Dis 1998;26:1–10.
[10] Landersdorfer CB, Nation RL. Limitations of antibiotic MIC-based PK-PD metrics: looking back to move forward. Front Pharmacol 2021;12:770518.
[11] Bulman ZP, Wicha SG, Nielsen EI, Lenhard JR, Nation RL, Theuretzbacher U, et al. Research priorities towards precision antibiotic therapy to improve patient care. Lancet Microbe 2022;3:e795–802.
[12] Bulitta JB, Shin E, Bergen PJ, Lang Y, Forrest A, Tsuji BT, et al. Distinguishing inducible and non-inducible resistance to colistin in *Pseudomonas aeruginosa* by quantitative and systems pharmacology modeling at low and standard inocula. J Pharm Sci 2024;113:202–13.
[13] Yusuf E, Van Herendael B, Verbrugghe W, Ieven M, Goovaerts E, Bergs K, et al. Emergence of antimicrobial resistance to *Pseudomonas aeruginosa* in the intensive care unit: association with the duration of antibiotic exposure and mode of administration. Ann Intensive Care 2017;7:72.
[14] Pelegrin AC, Palmieri M, Mirande C, Oliver A, Moons P, Goossens H, et al. *Pseudomonas aeruginosa*: a clinical and genomics update. FEMS Microbiol Rev 2021;45:fuab026.

[15] Hassuna NA, Darwish MK, Sayed M, Ibrahem RA. Molecular epidemiology and mechanisms of high-level resistance to meropenem and imipenem in *Pseudomonas aeruginosa*. Infect Drug Resist 2020;13:285–93.
[16] Patrier J, Timsit J-F. Carbapenem use in critically ill patients. Curr Opin Infect Dis 2020;33:86–91.
[17] Minichmayr IK, Aranzana-Climent V, Friberg LE. Pharmacokinetic/pharmacodynamic models for time courses of antibiotic effects. Int J Antimicrob Agents 2022;60:106616.
[18] Moya B, Dötsch A, Juan C, Blázquez J, Zamorano L, Haussler S, et al. Beta-lactam resistance response triggered by inactivation of a nonessential penicillin-binding protein. PLOS Pathog 2009;5:e1000353.
[19] Moya B, Zamorano L, Juan C, Pérez JL, Ge Y, Oliver A. Activity of a new cephalosporin, CXA-101 (FR264205), against beta-lactam-resistant *Pseudomonas aeruginosa* mutants selected *in vitro* and after antipseudomonal treatment of intensive care unit patients. Antimicrob Agents Chemother 2010;54:1213–7.
[20] Clinical and Laboratory Standards Institute. Performance standards for antimicrobial susceptibility testing, CLSI M100, CLSI M100. Wayne, PA: Clinical and Laboratory Standards Institute; 2023.
[21] Riera E, Cabot G, Mulet X, García-Castillo M, del Campo R, Juan C, et al. *Pseudomonas aeruginosa* carbapenem resistance mechanisms in Spain: impact on the activity of imipenem, meropenem and doripenem. J Antimicrob Chemother 2011;66:2022–7.
[22] Ehmann L, Zoller M, Minichmayr IK, Scharf C, Huisinga W, Zander J, et al. Development of a dosing algorithm for meropenem in critically ill patients based on a population pharmacokinetic/pharmacodynamic analysis. Int J Antimicrob Agents 2019;54:309–17.
[23] Burger R, Guidi M, Calpini V, Lamoth F, Decosterd L, Robatel C, et al. Effect of renal clearance and continuous renal replacement therapy on appropriateness of recommended meropenem dosing regimens in critically ill patients with susceptible life-threatening infections. J Antimicrob Chemother 2018;73:3413–22.
[24] Cojutti P, Sartor A, Righi E, Scarparo C, Bassetti M, Pea F. Population pharmacokinetics of high-dose continuous-infusion meropenem and considerations for use in the treatment of infections due to KPC-producing klebsiella pneumoniae. Antimicrob Agents Chemother 2017;61:e00794–17.
[25] Minichmayr I, Kappetein S, Brill M, Friberg L. Model-informed translation of *in vitro* effects of short-, prolonged- and continuous-infusion meropenem against *Pseudomonas aeruginosa* to clinical settings. Antibiotics (Basel) 2022;11:1036.
[26] Gatti M, Pea F. Continuous versus intermittent infusion of antibiotics in gram-negative multidrug-resistant infections. Curr Opin Infect Dis 2021;34:737–47.
[27] Roberts JA, Abdul-Aziz MH, Lipman J, Mouton JW, Vinks AA, Felton TW, et al. Individualised antibiotic dosing for patients who are critically ill: challenges and potential solutions. Lancet Infect Dis 2014;14:498–509.
[28] Abdul-Aziz MH, Alffenaar JC, Bassetti M, Bracht H, Dimopoulos G, Marriott D, et al. Antimicrobial therapeutic drug monitoring in critically ill adult patients: a position paper. Intensive Care Med 2020;46:1127–53.
[29] Guilhaumou R, Benaboud S, Bennis Y, Dahyot-Fizelier C, Dailly E, Gandia P, et al. Optimization of the treatment with beta-lactam antibiotics in critically ill patients – Guidelines from the French Society of Pharmacology and Therapeutics (Société Française de Pharmacologie et Thérapeutique—SFPT) and the French Society of Anaesthesia and Intensive Care Medicine (Société Française d'Anesthésie et Réanimation—SFAR). Crit Care 2019;23:104.
[30] Abdul-Aziz MH, Lipman J, Mouton JW, Hope WW, Roberts JA. Applying pharmacokinetic/pharmacodynamic principles in critically ill patients: optimizing efficacy and reducing resistance development. Semin Respir Crit Care Med 2015;36:136–53.
[31] López-Causapé C, Cabot G, del Barrio-Tofiño E, Oliver A. The versatile mutational resistome of *Pseudomonas aeruginosa*. Front Microbiol 2018;9:685.
[32] Tamber S, Ochs MM, Hancock RE. Role of the novel OprD family of porins in nutrient uptake in *Pseudomonas aeruginosa*. J Bacteriol 2006;188:45–54.
[33] Kos VN, Déraspe M, McLaughlin RE, Whiteaker JD, Roy PH, Alm RA, et al. The resistome of *Pseudomonas aeruginosa* in relationship to phenotypic susceptibility. Antimicrob Agents Chemother 2015;59:427–36.
[34] Jacobs M, Grégoire N, Couet W, Bulitta JB. Distinguishing antimicrobial models with different resistance mechanisms via population pharmacodynamic modeling. PLOS Comput Biol 2016;12:e1004782.
[35] Corona A, Palmer SO, Zamacona R, Mendez B, Dean FB, Bullard JM. Discovery and characterization of chemical compounds that inhibit the function of Aspartyl-tRNA synthetase from *Pseudomonas aeruginosa*. SLAS Discov 2018;23:294–301.
[36] Balboa S, Hu Y, Dean FB, Bullard JM. Lysyl-tRNA synthetase from *Pseudomonas aeruginosa*: characterization and identification of inhibitory compounds. SLAS Discov 2020;25:57–69.
[37] Wardell SJT, Rehman A, Martin LW, Winstanley C, Patrick WM, Lamont IL. A large-scale whole-genome comparison shows that experimental evolution in response to antibiotics predicts changes in naturally evolved clinical *Pseudomonas aeruginosa*. Antimicrob Agents Chemother 2019;63:e01619–19.
[38] Vasala A, Hytonen VP, Laitinen OH. Modern tools for rapid diagnostics of antimicrobial resistance. Front Cell Infect Microbiol 2020;10:308.
[39] Haag S, Häussler S. Quo vadis clinical diagnostic microbiology? Clin Microbiol Infect 2021;27:1562–4.
[40] Bonine NG, Berger A, Altincatal A, Wang R, Bhagnani T, Gillard P, et al. Impact of delayed appropriate antibiotic therapy on patient outcomes by antibiotic resistance status from serious gram-negative bacterial infections. Am J Med Sci 2019;357:103–10.
[41] Wenzler E, Maximos M, Asempa TE, Biehle L, Schuetz AN, Hirsch EB. Antimicrobial susceptibility testing: an updated primer for clinicians in the era of antimicrobial resistance: insights from the Society of Infectious Diseases Pharmacists. Pharmacotherapy 2023;43:264–78.
[42] Cortes-Lara S, Barrio-Tofiño ED, López-Causapé C, Oliver A, Martínez-Martínez L, Bou G, et al. Predicting *Pseudomonas aeruginosa* susceptibility phenotypes from whole genome sequence resistome analysis. Clin Microbiol Infect 2021;27:1631–7.
[43] Iyobe S, Watanabe M, Mitsuhashi S, Inoue M. Estimation of outer membrane permeability of carbapenem antibiotics to *Pseudomonas aeruginosa*. J Infect Chemother 1999;5:168–70.

Please cite this article as: Fuhs DT et al., The effects of single and multiple resistance mechanisms on bacterial response to meropenem, Clinical Microbiology and Infection, https://doi.org/10.1016/j.cmi.2024.06.026